

Chinese Science Bulletin 2005 Vol. 50 No. 18 1995—1998

## ***In situ* time-resolved FTIRS study of adsorption and oxidation of ethylene glycol on Pt(100) electrode**

FAN Youjun, ZHOU Zhiyou, FAN Chunjie, ZHEN Chunhua, CHEN Shengpei & SUN Shigang

State Key Laboratory of Physical Chemistry of Solid Surfaces, Department of Chemistry, Xiamen University, Xiamen 361005, China  
Correspondence should be addressed to Sun Shigang (email: sgsun@xmu.edu.cn)

**Abstract** Adsorption and oxidation of ethylene glycol (EG) on Pt(100) electrode were studied by *in situ* time-resolved FTIRS (TRFTIRS). The TRFTIR spectra recorded at 0.10 V illustrate that an IR band appears near 2050  $\text{cm}^{-1}$  at  $t > 5$  s, corresponding to linearly bonded CO formed in dissociative adsorption of EG. The TRFTIR results have confirmed also that CO species are distributed uniformly on Pt(100) surface. Another band appears near 2342  $\text{cm}^{-1}$  at  $t > 70$  s, associating with IR absorption of  $\text{CO}_2$  produced in the direct oxidation of EG. With the increase of electrode potential, the direct oxidation of EG becomes gradually the main reaction. When the potential is above 0.40 V, the oxidation of EG occurs mainly via the reactive intermediates, i.e. species containing  $-\text{COOH}$  determined by *in situ* TRFTIRS.

**Keywords:** ethylene glycol, Pt(100) electrode, dissociative adsorption and oxidation, *in situ* time-resolved FTIR spectroscopy.

DOI: 10.1360/982004-540

Metal single crystal planes provide model electrocatalysts of well-defined surface structure, and play an important role in fundamental studies of electrocatalysis. Ethylene glycol (EG) has attracted considerable interests in both basic studies and applications in direct fuel cells, since its complete oxidation transfers 10 electrons. In the strong acid environment of proton exchange membrane fuel cell (PEMFC), the sole stable and most active metal catalyst for the electro-oxidation of alcohols is platinum<sup>[1]</sup>. Extensive efforts have been devoted to investigating electrochemical adsorption and oxidation properties of EG on Pt electrodes with different surface structures<sup>[2-17]</sup>. The results demonstrated that the electrocatalytic oxidation of EG on Pt electrode occurred via a dual path reaction mechanism, and its oxidation includes a set of consecutive and parallel steps yielding several C1- and C2-products<sup>[4-6,9]</sup>. The oxidation route of EG proceeding without C-C bond cleavage in acidic solutions includes consecutive, two-electron transferring processes that yield some intermediates, such as glycolaldehyde, glyoxal, glycolic acid, glyoxylate and oxalic acids, and the final product is  $\text{CO}_2$ . In parallel to the above route, the dissociative ad-

sorption of EG may occur due to the strong interaction between EG and Pt surface, resulting in formation of adsorbed CO species and other strongly bound adsorbates, which empoids Pt surface and causes the so-called “self-poisoning” phenomenon. However, these studies were focused mainly on surface structure effects of Pt electrodes and on the reaction mechanism by determining intermediates and products involved in EG electrocatalytic oxidation using different methods, such as chromatography<sup>[9,12]</sup>, *in situ* FTIR spectroscopy<sup>[2,3,6,10,12,13]</sup>, and differential electrochemical mass spectroscopy<sup>[10]</sup>, and the surface processes and kinetics of EG oxidation were less studied and needed to be further understood at a molecular level. In the present paper, the dissociative adsorption and oxidation of EG on Pt(100) surface are investigated by *in situ* time-resolved FTIR reflection spectroscopy, and new information of EG reaction kinetics was obtained.

### 1 Experimental

*In situ* time-resolved FTIR spectroscopy experiments were carried out on a Nexus 870 FTIR apparatus (Nicolet) equipped with a liquid nitrogen cooled MCT-A detector. 10 interferograms were collected and co-added into each spectrum of spectral resolution 16  $\text{cm}^{-1}$ . The resulting spectrum is calculated as  $\Delta R / R = (R_{E_2} - R_{E_1}) / R_{E_1}$ , where  $R_{E_1}$  and  $R_{E_2}$  are single-beam spectra recorded at  $E_1$  and  $E_2$ , respectively. A saturated calomel electrode (SCE) was used as reference electrode. Before each measurement the Pt(100) electrode was annealed in a hydrogen-oxygen flame, quenched with super pure water and transferred into electrochemical cell under protection of a droplet of pure water. The solutions were prepared using Millipore water (18.0  $\text{M}\Omega \text{ cm}$ ) provided from a Milli-Q Lab apparatus (Nihon Millipore), super pure  $\text{H}_2\text{SO}_4$  and ethylene glycol of analytical grade (both from Shanghai Chemicals, Inc., China). All measurements were carried out at around 20 °C.

### 2 Results and discussion

Our previous studies<sup>[18]</sup> illustrated that the average rate ( $\bar{v}$ ) of dissociative adsorption of EG on Pt(100) electrode varies with adsorption potential  $E_{\text{ad}}$  following a volcano-type distribution. The maximum of  $\bar{v}$  ( $\bar{v}^{\text{max}}$ ) is located near 0.10 V. Taking  $E_{\text{ad}} = 0.10$  V as a coteau,  $\bar{v}$  declines no matter whether  $E_{\text{ad}}$  decreases or increases gradually.  $\bar{v}$  tends towards zero when the adsorption potential is below  $-0.22$  V or above 0.40 V.

*In situ* time-resolved FTIR spectra (TRFTIRS) obtained on Pt(100) electrode at  $E_2 = 0.10, 0.25, 0.40$  and 0.90 V in 0.1  $\text{mol L}^{-1}$  EG + 0.1  $\text{mol}\cdot\text{L}^{-1}$   $\text{H}_2\text{SO}_4$  solution are shown in Fig. 1(a)–(d). We can see from Fig. 1(a) that a negative going band near 2050  $\text{cm}^{-1}$  starts to appear in the spectrum at  $t > 5$  s, corresponding to linearly bonded CO

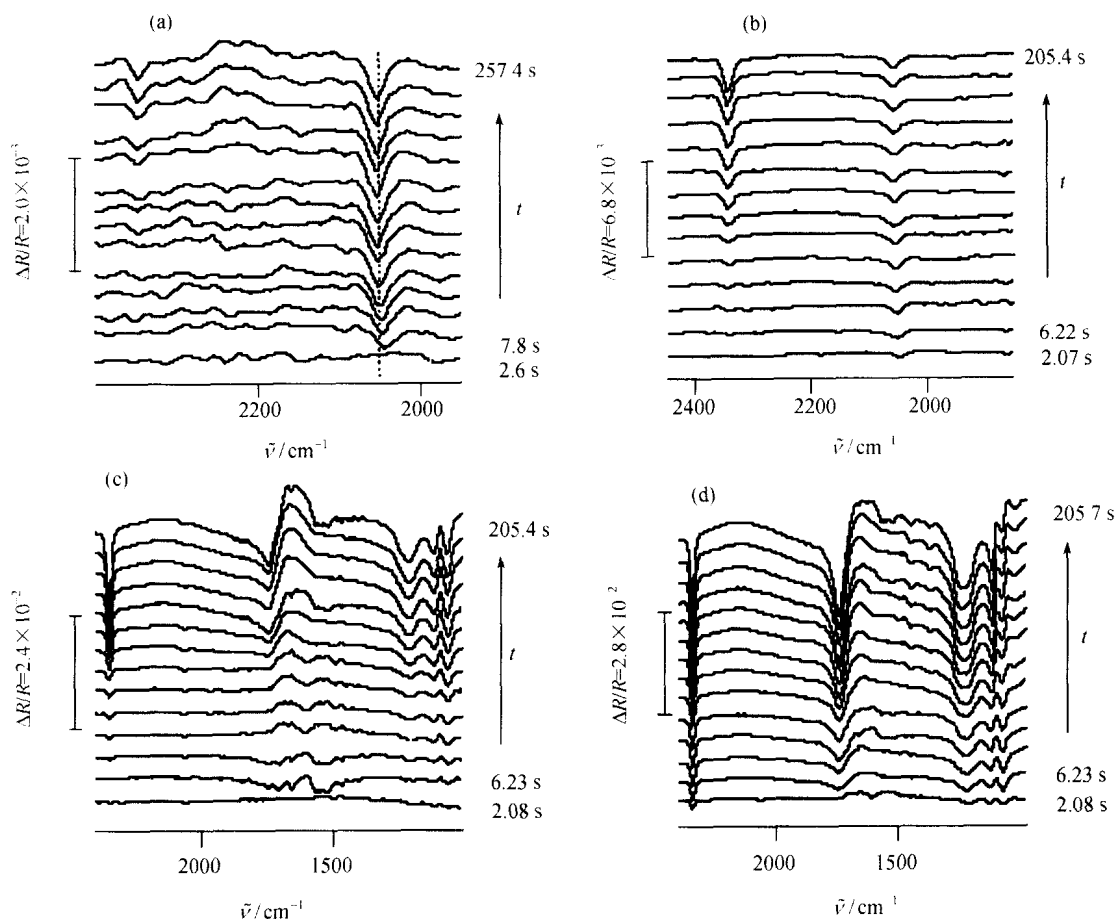


Fig. 1. *In situ* time-resolved FTIR spectra obtained for Pt(100) electrode in 0.1 mol·L<sup>-1</sup> EG + 0.1 mol·L<sup>-1</sup> H<sub>2</sub>SO<sub>4</sub> solution with  $E_1$  at -0.22 V and  $E_2$  at (a) 0.10 V, (b) 0.25 V, (c) 0.40 V, (d) 0.90 V.

(CO<sub>L</sub>) derived from dissociative adsorption of EG on Pt(100) electrode at  $E_2 = 0.10$  V<sup>[2,3,6]</sup>. The intensity of the band increases progressively with time and attains almost a constant value at  $t > 100$  s. The negative going monopolar band and its variation indicate that the dissociative adsorption of EG on Pt(100) electrode at  $E_1 = -0.22$  V has not occurred (otherwise a bipolar band will appear), and CO<sub>L</sub> species were formed exclusively at 0.10 V. The intensity of the band increases progressively with  $t$ , indicating that the quantity of CO<sub>L</sub> increases gradually and it is accumulated on Pt(100) surface. The band center ( $\tilde{\nu}_{\text{CO}_L}$ ) shifts positively with time from 2042 cm<sup>-1</sup> ( $t = 7.8$  s) to 2054 cm<sup>-1</sup> ( $t = 257.4$  s), which is apparently caused by the increase of CO<sub>L</sub> coverage, and demonstrates that the CO<sub>L</sub> species are distributed uniformly on Pt(100) surface without the formation of island. At the same time, a small negative going band near 2342 cm<sup>-1</sup> appears when  $t > 70$  s, corresponding to the asymmetry stretching of CO<sub>2</sub> that is the final product of EG direct oxidation<sup>[3, 6]</sup>. The intensity of this band increases progressively with  $t$ . The appearance of CO<sub>2</sub> band indicates that EG can be directly oxi-

dized at 0.10 V where is located the maximum value of  $\bar{v}$  in its volcano-type distribution, and illustrates the competitive reaction with EG dissociative adsorption. Fig. 2(a) shows the variation of the integration intensity of CO<sub>L</sub> and CO<sub>2</sub> bands with  $t$  on Pt(100) surface for  $E_2 = 0.10$  V. We can see that the formation of CO<sub>L</sub> on Pt(100) surface in EG dissociative adsorption is obviously more significant than the production of CO<sub>2</sub> species in EG direct oxidation.

In Fig. 1(b) ( $E_2 = 0.25$  V), we can observe two similar IR bands, namely, CO<sub>L</sub> band at about 2050 cm<sup>-1</sup> and CO<sub>2</sub> band around 2342 cm<sup>-1</sup>. The intensity of CO<sub>L</sub> band still increases with increasing  $t$  and rapidly attains a stable constant value, and in the initial stage of reaction the band center ( $\tilde{\nu}_{\text{CO}_L}$ ) also shifts positively with increasing  $t$ . In contrast to the results in Fig. 1(a), the CO<sub>2</sub> band appears in the initial stage of reaction, its intensity increases faster with increasing  $t$  than that of CO<sub>L</sub> band. The variation of integration intensity of CO<sub>L</sub> and CO<sub>2</sub> bands with  $t$  at this potential is shown in Fig. 2(b). We can see that in the recorded time window, the intensity of CO<sub>2</sub> band increases

linearly and quickly with increasing  $t$ , and the variation of  $\text{CO}_L$  band intensity with  $t$  is similar to that of  $E_2 = 0.10$  V. We can see also that when  $t$  is larger than 60 s, the intensity of  $\text{CO}_2$  band becomes stronger than that of the  $\text{CO}_L$  band.

When  $E_2 = 0.40$  V (Fig. 1(c)), the number of IR bands is increased and all bands are negatively going. Except the  $\text{CO}_L$  and  $\text{CO}_2$  bands, the assignment of other bands is as follows: the bands near  $1740$  and  $1230$   $\text{cm}^{-1}$  may be attributed to IR absorption of  $-\text{COOH}$  groups<sup>[4]</sup>; the band near  $1100$   $\text{cm}^{-1}$  can be assigned to the stretching vibration of  $\text{SO}_4^{2-}$  anions<sup>[19]</sup>; the band near  $1059$   $\text{cm}^{-1}$  can be ascribed to C—O stretching of the primary alcohol<sup>[4]</sup>. Among these bands, the intensity of the  $-\text{COOH}$  and the

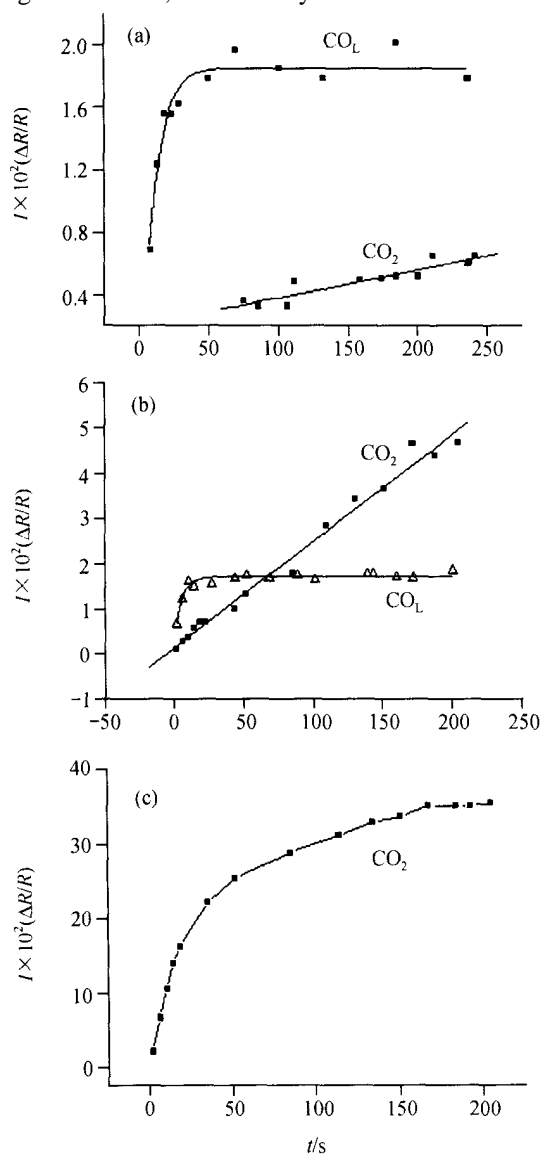


Fig. 2. Comparison of variation of integration intensity ( $I$ ) of  $\text{CO}_L$  and  $\text{CO}_2$  band versus reaction time  $t$ . (a)  $E_2 = 0.10$  V; (b)  $E_2 = 0.25$  V; (c)  $E_2 = 0.75$  V.

$\text{CO}_2$  bands is gradually increased with increasing  $t$ , and is apparently larger than that measured at  $E_2 = 0.25$  V. This may indicate that the rate of EG direct oxidation increases significantly at  $E_2 = 0.40$  V, accordingly, the production of intermediates containing  $-\text{COOH}$  and  $\text{CO}_2$  in EG oxidation on Pt(100) is fast at this potential. We can also see that the intensity of IR bands near  $1100$  and  $1059$   $\text{cm}^{-1}$  is gradually increased with increasing  $t$ , which may be attributed to the consumption of  $\text{H}_2\text{O}$  in the thin-layer solution involved in EG oxidation. In addition, the  $\text{CO}_L$  band can be hardly observed in the spectra, which may be attributed to three aspects: (1) The rate of EG dissociative adsorption is very small at this potential<sup>[18]</sup>; (2) the adsorbed CO derived from EG dissociative adsorption can be oxidized, which decreases the possibility of  $\text{CO}_{ad}$  accumulation on Pt(100) surface; (3) the competition occurs between dissociative adsorption and direction oxidation of EG, the latter takes place via the reactive intermediates, i.e. species containing  $-\text{COOH}$  determined by *in situ* TRFTIRS. With further increase of sample potential  $E_2$  (Fig. 1(d)), the intensity of the above IR bands is increased rapidly with increasing  $t$ , which can be clearly seen from *in situ* TRFTIR spectra of different  $E_2$  but at the same reaction time ( $t = 60$  s) shown in Fig. 3. From the variation of integration intensity of  $\text{CO}_2$  band with  $t$  at  $E_2 = 0.75$  V given in Fig. 2(c), we can see that when  $t$  is longer than 100 s, the quantity of  $\text{CO}_2$  produced by EG oxidation approaches to a stable value. At this potential no  $\text{CO}_{ad}$  species can be detected by *in situ* TRFTIRS.

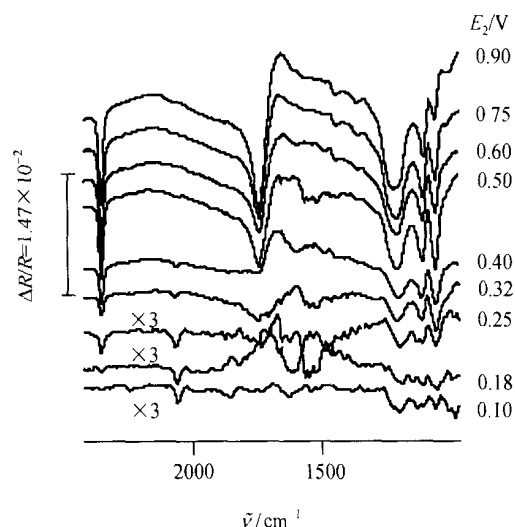


Fig. 3. *In situ* time-resolved FTIR Spectra recorded on Pt(100) electrode for reaction time  $t = 60$  s in  $0.1 \text{ mol}\cdot\text{L}^{-1}$  EG +  $0.1 \text{ mol}\cdot\text{L}^{-1}$   $\text{H}_2\text{SO}_4$  solution with  $E_1$  at  $-0.22$  V and varying  $E_2$  (0.10, 0.18, 0.25, 0.32, 0.40, 0.50, 0.60, 0.75, 0.90 V).

### 3 Conclusion

In the present paper, the adsorption and oxidation of ethylene glycol (EG) on Pt(100) electrode were studied by *in situ* time-resolved FTIRS. The results demonstrated that

## ARTICLES

a negative going band near  $2050\text{ cm}^{-1}$  corresponding to linearly bonded CO ( $\text{CO}_L$ ) formed mainly via dissociative adsorption of EG at  $E_2 = 0.10\text{ V}$ , and this band appears in the spectra at reaction time  $t > 5\text{ s}$ . The intensity of this band is increased progressively with increasing  $t$ . In the initial stage, the  $\text{CO}_L$  band center ( $\tilde{\nu}_{\text{CO}_L}$ ) is blue-shifted with increasing  $t$ , indicating that the  $\tilde{\nu}_{\text{CO}_L}$  changes with  $\text{CO}_L$  coverage, and implying that  $\text{CO}_L$  species are distributed uniformly on Pt(100) surface. In addition, a band near  $2342\text{ cm}^{-1}$  appears in the spectra at  $t > 70\text{ s}$ , which is assigned to IR absorption of  $\text{CO}_2$  species that are formed via direct oxidation of EG. With the increase of  $E_2$ , the direct oxidation of EG becomes gradually the main route of EG oxidation, and leads to the decrease of the rate of EG dissociative adsorption on Pt(100) surface. When  $E_2 > 0.40\text{ V}$ , all EG molecules reaching electrode surface can be oxidized directly into  $\text{CO}_2$ , and the oxidation of EG occurs mainly via the reactive intermediates that are the species containing  $-\text{COOH}$  determined by *in situ* TRFTIRS.

**Acknowledgements** This work was supported by the National Natural Science Foundation of China (Grant Nos. 20373059 and 90206039) and the "973" Program (Grant No. 2002CB211804).

### References

1. Lamy, C., Lima, A., LeRhun, V. et al., Recent advances in the development of direct alcohol fuel cell (DAFC), *J. Power Sources*, 2002, 105: 283–296.
2. Hahn, F., Beden, B., Kadirgan, F. et al., Electrocatalytic oxidation of ethylene glycol: Part III. *In-situ* infrared reflectance spectroscopic study of the strongly bound species resulting from its chemisorption at a platinum electrode in aqueous medium, *J. Electroanal. Chem.*, 1987, 216: 169–180.
3. Christensen, P. A., Hamnett, A., The oxidation of ethylene glycol at a platinum electrode in acid and base: An *in situ* FTIR study, *J. Electroanal. Chem.*, 1989, 260: 347–359.
4. Chen, A. C., Sun, S. G., *In situ* FTIR reflection spectroscopic studies of adsorption and oxidation of ethylene glycol on Pt electrode (I) acidic media, *Chem. J. Chinese Univ.* (in Chinese), 1994, 15(3): 401–405.
5. Chen, A. C., Sun, S. G., *In situ* FTIR reflection spectroscopic studies of adsorption and oxidation of ethylene glycol on Pt electrode (II) alkaline media, *Chem. J. Chinese Univ.* (in Chinese), 1994, 15(4): 548–551.
6. Wieland, B., Lancaster, J. P., Hoaglund, C. S. et al., Electrochemical and infrared spectroscopic quantitative determination of the Platinum-catalyzed ethylene glycol oxidation mechanism at CO adsorption potentials, *Langmuir*, 1996, 12: 2594–2601.
7. Horányi, G., Kazarinov, V. E., Vassiliev, Y. B. et al., Electrochemical and adsorption behaviour of ethylene glycol and its oxidative derivatives at platinum electrodes: Part II. Electrocatalytic transformations under steady-state experimental conditions at a platinumized platinum electrode in acid medium, *J. Electroanal. Chem.*, 1983, 147(1-2): 263–278.
8. Lebedeva, N. P., Kryukova, G. N., Tsybulya, S. V. et al., Effects of microstructure in ethylene glycol oxidation on graphite supported platinum electrodes, *Electrochim. Acta*, 1998, 44(8-9): 1431–1440.
9. Cherstiouk, O. V., Savinova, E. R., Kozhanova, L. A. et al., Electrocatalytic oxidation of ethylene glycol on dispersed Pt: Determination of the reaction products, *React. Kinet. Catal. Lett.*, 2000, 69(2): 331–338.
10. Gootzen, J. F. E., Visscher, W., Vanveen, J. A. R., Characterization of ethanol and 1,2-ethanediol adsorbates on platinumized platinum with Fourier transform infrared spectroscopy and differential electrochemical mass spectrometry, *Langmuir*, 1996, 12(21): 5076–5082.
11. Beltowska-Brzezinska, M., Luczak, T., Holze, R., Electrocatalytic oxidation of mono- and polyhydric alcohols on gold and platinum, *J. Appl. Electrochem.*, 1997, 27: 999–1011.
12. Dailey, A., Shin, J., Korzeniewski, C., Ethylene glycol electrochemical oxidation at platinum probed by ion chromatography and infrared spectroscopy, *Electrochim. Acta*, 1998, 44: 1147–1152.
13. Gootzen, J. F. E., Wonders, A. H., Cox, A. P. et al., On the adsorbates formed during the platinum catalyzed (electro)oxidation of ethanol, 1,2-ethanediol and methyl- $\alpha$ -D-glucopyranoside at high pH, *J. Mol. Catal. A: Chem.*, 1997, 127(1-3): 113–131.
14. Orts, J. M., Fernandez-Vega, A., Feliu, J. M. et al., Electrochemical oxidation of ethylene glycol on Pt single crystal electrodes with basal orientations in acidic medium, *J. Electroanal. Chem.*, 1990, 290(1-2): 119–133.
15. Markovic, N. M., Avramov-Ivic, M. L., Marinkovic, N. S. et al., Structural effects in electrocatalysis: Ethylene glycol oxidation on platinum single-crystal surfaces, *J. Electroanal. Chem.*, 1991, 312(1-2): 115–130.
16. Sun, S. G., Chen, A. C., Huang, T. S. et al., Electrocatalytic properties of Pt(111), Pt(332), Pt(331) and Pt(100) single crystal electrodes towards ethylene glycol oxidation in sulphuric acid solutions, *J. Electroanal. Chem.*, 1992, 340: 213–226.
17. Sun, S. G., Chen, A. C., Effects of ethylene glycol (EG) concentration and pH of solutions on electrocatalytic properties of Pt(111) electrode in EG oxidation – a comparison study with adjacent planes of platinum single crystal situated in [110] and [011] crystallographic zones, *Electrochim. Acta*, 1994, 39(7): 967–973.
18. Fan, Y. J., Zhou, Z. Y., Zhen, C. H. et al., Kinetics of dissociative adsorption of ethylene glycol on Pt(100) electrode surface in sulfuric acid solutions, *Electrochim. Acta*, 2004, 49: 4659–4666.
19. Iwasita, T., Nart, F. C., *In situ* infrared spectroscopy at electrochemical interfaces, *Progr. Surf. Sci.*, 1997, 55: 271–340.

(Received October 29, 2004; accepted March 21, 2005)